WATER-LAYER-RELATED DEMULTIPLE METHOD USING CONSTRAINTS IN THE SPARSE, LOCAL TAU-P DOMAIN

WEIQIANG SUN and HUAZHONG WANG

Wave Phenomena and Inversion Imaging Group (WPI), School of Ocean and Earth Science, Tongji University, Shanghai 200092, P.R. China. tswq_123456@msn.com

(Received December 3, 2015; revised version accepted July 22, 2016)

ABSTRACT

Sun, W. and Wang, H., 2016. Water-layer-related demultiple method using constraints in the sparse, local tau-p domain. *Journal of Seismic Exploration*, 25: 463-483.

Water-layer-related multiple suppression remains a challenge in marine data processing. Surface-related multiple elimination (SRME) is proven to be effective in many offshore cases. As an alternative to SRME, model-based water-layer demultiple offers an effective way to predict water-layer-related multiples. In both SRME and model-based water-layer demultiple methods, the multiple contribution gather plays an important role in multiple prediction. In this paper, we propose a method to predict and subtract the water-layer-related multiples in the local tau-p domain. The sparse local tau-p transform is implemented by a weighted least-squares inversion with weights in the local tau-p domain, yielding higher resolution. Being in the local tau-p domain, the seismic data and the Green's functions of the water-layer primary reflections can be combined such that the true downward reflection points for different water-layer-related multiple generators are automatically selected by obeying Snell's law. In this way, the accuracy of water-layer-related multiple prediction is improved. In addition, it is proposed to replace the traditional adaptive subtraction by a filtering in the local tau-p domain, where the semblance of the predicted water-layer-related multiples can be used as constraints to identify the locations of water-layer-related multiples. Subsequently, a Butterworth-type filter can be designed to adaptively subtract the predicted water-layer-related multiples from the tau-p transformed input data. Compared with the conventional methods for adaptive subtraction via the L_2-norm, our proposed method is more effective when the primaries and water-layer-related multiples are correlated. The constraints of the semblance not only provide an effective and robust way for amplitude matching, but also weaken the effects of distorted wavelets in subtraction. Our synthetic and field data examples show that the proposed flow of first predicting water-layer-related multiples and, second, separating them from the primaries by utilizing the sparse local tau-p transform enhances the water-layer-related multiple suppression results.

KEY WORDS: water-layer-related multiple, sparse local tau-p transform,
multiple contribution gather optimization, adaptive subtraction, semblance.

0963-0651/16/$5.00

INTRODUCTION

The suppression of multiple reflections has been a longstanding problem in offshore seismic data processing. An important class of the techniques is formed by wave-equation-based methods which suppress the multiples through wavefield prediction and subtraction.

In the prediction stage, most methods focus on the prediction of the kinematic characteristics, such as the traveltime of the multiples. The data-driven surface-related multiple elimination (SRME) method (Berkhout and Verschuur, 1997) has been proven effective in many offshore cases. SRME simultaneously predicts all types of surface-related multiples without using any prior information of the subsurface. The information hidden in the seismic data is exploited by SRME. However, the near-offset data are missing due to instrumental setups, and both the primaries and multiples are weak and often contaminated by other arrivals such as direct, head and refracted waves (Sun and Wang, 2014). All these factors make the data-driven methods less effective in shallow water cases. Besides, iterative SRME suffers from inconsistency between prediction and subtraction when the water depth is shallow or the sea-floor is hard. That is, different orders of multiples require different amplitude corrections even with a perfect sampling or recorded near-offset data. Apart from SRME, MPI (Wang, 2004, 2007) predicts the multiples through data-driven inversion. Compared with SRME, the MPI demultiple technique minimizes the edge effects and eliminates the needs for near-offset traces.

Model-based methods (Berryhill and Kim, 1986; Wiggins, 1988) relieve the dependence on completeness of data. With the prior information of the water-layer model, model-based methods can effectively predict the water-layer-related multiples (WLRM). Lokshtanov (1999) proposes a consistent wave-equation-based method for simultaneous prediction of both source- and receiver-side WLRMs. Based on Lokshtanov's method, deterministic water-layer-related demultiple (DWD) (Moore et al., 2006) uses an operator, deterministically designed from a water-layer model picked from the autocorrelation, to predict the WLRMs. Model-based water-layer demultiple (MWD) (Wang et al., 2011) is an alternative to SRME for WLRM prediction. In MWD, the water-layer primary reflections are replaced by the water-layer Green's functions to convolve with the recorded data. Compared with the conventional SRME, MWD removes the crosstalks between different orders of multiples, and the spectrum distortion caused by the extra source wavelet is also attenuated.

All the convolution-based methods for multiple prediction, either SRME or MWD, involve the convolutions of the traces from a common shot gather (CSG) with a common receiver gather (CRG) to form the multiple contribution gather (MCG), the stack of which predicts the surface-related multiples or

WLRMs. Within the MCG, most contributions are related to non-physical events, which will be stacked out by destructive interference. Only a small portion of the MCG that contains the true downward reflection points (DRP) contributes constructively to the prediction of multiples. However, the right stacking aperture is usually not known in advance. Bienati (2012) proposes a method to automatically define the stacking aperture in 3D SRME. Keydar et al. (1998) proposes a method to predict the multiples kinematically relying on the angle relationship. Verschuur et al. (2007) separates the reflections and diffractions in the tau-p domain, and separately predicts the diffracted multiples. Donno (2010) presents a SRME-based approach to improve the prediction of the surface-related multiples in the curvelet domain. The curvelet transform is used to decompose the seismic data into local plane waves. The directionality of curvelets is utilized to optimize the MCG. Similar to this idea, the method presented in this paper focuses on both the MCG optimization through exploitation of the Snell's law and WLRM prediction in the local tau-p domain. The sparse local tau-p transform is implemented by a weighted least-squares inversion. The resolution is higher than the conventional local tau-p transform via slant stack. In the local tau-p domain, the recorded data are convolved with the Green's functions of water-layer primary reflections. They are combined such that the true DRPs for different WLRM generators are automatically selected by obeying Snell's law. This results in better WLRM prediction. The proposed procedure can be implemented in both SRME and MWD process, but in this paper it is demonstrated for the MWD situation.

Although the kinematic information of the multiples can be predicted, the dynamic characteristics cannot be predicted accurately due to the effects of modeling inaccuracy and noise contamination. Multiple subtraction compensates for amplitude and phase discrepancies that arise from the process of multiple prediction. The subtraction is usually posed as a least-squares minimization problem that minimizes the energy difference between the recorded data and the predicted multiples, which is implemented as single or multi-channel Wiener filtering. However, the primaries are assumed to have minimum energy and to be orthogonal to the multiples, as required by the L_2-norm (Guitton and Verschuur, 2004). Some problems arise when these two assumptions are not met. Besides the amplitude attributes, pseudo-multichannel matching filter takes into account residual traveltime and phase in the process of subtraction (Monk, 1993; Wang, 2003). When the primaries and multiples are not orthogonal, the primaries overlapping the multiples will be wrongly subtracted. To overcome this problem, Spitz (1999) proposed a 'pattern recognition' subtraction method based on the prediction error filter (PEF). The subtraction methodology is concerned with the patterns (shapes) of the events. The pattern of the event is defined as the spatial vector that contains the phase shift and lateral amplitude variation from trace to trace but excludes the waveform of the event. Independent component analysis treats the problem as "blind source separating" issues. The separation of multiples and primaries relies on higher-order statistics, which are utilized to measure the dependence between these components (Lu and Liu, 2007). These methods have partly succeeded in breaking through the orthogonality assumption. Considering the L1-norm is less sensitive to outliers, it is used as an alternative to the L_2-norm to avoid the assumption that primaries should have minimum energy (Guitton and Verschuur, 2004). More recently, the curvelet domain has been used to adaptively subtract the multiples (Herrmann et al., 2008; Wu and Barry, 2013). The method supposes that primaries and multiples map into different positions in the curvelet domain because of different local slopes or frequency contents. Van Groenestijn and Verschuur (2008) present a method to estimate the primaries through sparse inversion (EPSI) by redefining SRME as a large-scale inversion process. Recently, the ghost effect is included into EPSI to generate better primary estimation (Verschuur, 2013).

In this paper, the following adaptive subtraction of WLRMs is also in the local tau-p domain. The primaries and multiples separate better in the local tau-p domain than they do in the space-time domain. And the adaptive filter becomes explicitly angle-dependent in the local tau-p domain. As the proposed prediction method can predict the traveltime of the multiples, the semblance of the predicted WLRMs can be used as constraints to identify the locations of WLRMs in the local tau-p domain. Hereby, a Butterworth-type filter can be designed to complete the adaptive subtraction. There are three advantages of the proposed method for adaptive subtraction. First, the predicted WLRMs can be effectively subtracted when they are not orthogonal to the primaries, and the primaries can be preserved at the same time. Second, the predicted multiples can be subtracted through filtering in the local tau-p domain rather than solving linear equations in a certain norm. Third, this method not only preserves the energy of the primaries but also weakens the sensitivity of wavelets on the subtraction at the same time.

The paper is organized as follows. In the next section, we illuminate the theory of the sparse local tau-p transform. In the following two sections, we propose a method for WLRM prediction and subtraction in the local tau-p domain, respectively. Finally, we test the proposed method through 2D synthetic and field examples.

THEORY and METHOD

Sparse local tau-p transform

Both multiple prediction and subtraction are implemented in the local tau-p domain. Thus a sparse local tau-p transform is required. Many papers have been devoted to the high-resolution Radon or tau-p transform (Trad et al., 2003). In the proposed method, the local tau-p transform is implemented by a weighted least-squares inversion with weights in the local tau-p domain, yielding higher resolution.

In the frequency domain, the forward problem of the local tau-p transform can be written as:

$$\begin{bmatrix} d_1 \\ d_2 \\ \vdots \\ d_m \end{bmatrix} = \begin{bmatrix} e^{i\omega p_1(x_1-x_0)} & e^{i\omega p_2(x_1-x_0)} & \cdots & e^{i\omega p_{n_p}(x_1-x_0)} \\ e^{i\omega p_1(x_2-x_0)} & e^{i\omega p_2(x_2-x_0)} & \cdots & e^{i\omega p_{n_p}(x_2-x_0)} \\ \vdots & \vdots & \ddots & \vdots \\ e^{i\omega p_1(x_m-x_0)} & e^{i\omega p_2(x_m-x_0)} & \cdots & e^{i\omega p_{n_p}(x_m-x_0)} \end{bmatrix} \begin{bmatrix} s_1 \\ s_2 \\ \vdots \\ s_{n_p} \end{bmatrix} , \tag{1}$$

where ω is the angular frequency. In the frequency domain, d_i is the input data, m is the number of traces in the spatially local window. x_i are the spatial locations of the input data, and x_0 is the reference trace, which is usually the central trace in the local window. p_{i_p} is the i_p-th ray parameter, n_p is the number of ray parameters. s_{i_p} is the local plane wave with the ray parameter being p_{i_p}.

The local tau-p transform is considered as an inversion problem. A common approach for obtaining a sparse local tau-p transform is to choose a L_1-norm for the model and a L_2-norm for the data misfit (Trad et al., 2003). The objective to be minimized can be written as:

$$J = \|\mathbf{As} - \mathbf{x}\|_2^2 + \lambda\|\mathbf{s}\| , \tag{2}$$

where matrix **A** consists of the basis functions corresponding to each ray parameter, and vector **s** and vector **x** are the data in the local plane wave domain and the spatially local input data in the space-time domain, respectively. And λ is the regularization parameter. The mixed norm problem can be easily transformed to a L_2-L_2-norm problem by using a weighted diagonal matrix **W**, in which the model-dependent elements on the diagonal are defined as:

$$w_{i_p,i_p} = 1/\sqrt{s} , \tag{3}$$

where w_{i_p,i_p} is the i_p-th element on the diagonal of matrix **W**. In this way, the sparse local tau-p transform can be implemented by a weighted least-squares problem. We utilize the energy of the data in the local plane wave domain to generate the weighted matrix. Although the tau-p-transformed data generated by the slant stack suffer from the leaking noise and low resolution, their energies can be utilized to evaluate the solution to the inverse problem. The larger the energy is, the more likely it is the true component in the local tau-p domain. Otherwise, the smaller the energy is, the more likely it is the leaking noise. The energy of the data in the local plane wave domain is defined as:

$$e(i_p) = \sum_{\omega_2}^{\omega_1} |s_0(i_p,\omega)|^2 \quad , \tag{4}$$

where $e(i_p)$, $i_p = 1,2,\cdots,n_p$ are the energies of the data in the local plane wave domain corresponding to the i_p-th ray parameter. ω_1 and ω_2 are the beginning and end of the frequency, respectively. $s_0(i_p,\omega)$, $i_p = 1,2,\cdots,n_p$ are the data in the local $p-\omega$ domain generated by the slant stack. Using $e(i_p)$ as weights, the weighted objective function to be minimized can be written as:

$$J = \|\mathbf{As} - \mathbf{x}\|_2^2 + \|\mathbf{Rs}\| \quad , \tag{5}$$

where matrix $\mathbf{R}$ is a diagonal $n_p \times n_p$ matrix, and the elements on the diagonal can be written as:

$$r_{i_p,i_p} = \lambda/\sqrt{e(i_p)} \quad , \tag{6}$$

where r_{i_p,i_p} is the i_p-th element on the diagonal. The solution to eq. (5) is:

$$\mathbf{S} = (\mathbf{A}^H\mathbf{A} + \mathbf{R})^{-1}\mathbf{A}^H\mathbf{x} \quad , \tag{7}$$

where the symbol H represents conjugate transpose. Neglecting the $(A^HA+R)^{-1}$, we achieve the results of the slant stack, i.e., A^HX. When $e(i_p)$ is large, r_{i_p,i_p} is small. The inverse of A^HA dominates the solution, and the resolution of A^HX is enhanced. When $e(i_p)$ is small, r_{i_p,i_p} is large. The inverse of r_{i_p,i_p} dominates the solution, and the leaking noise is suppressed. As a result, a sparse local tau-p transform is obtained.

Fig. 1 draws a comparison between slant stack and the sparse local tau-p transform. Panels in the top row compare the results of the forward local tau-p transform. Compared with a slant stack, the local tau-p transform generated by the proposed method has higher resolution. Besides, the leaking noise of slant stack contaminates signals. As the basis functions of the local tau-p transform do not form an orthogonal basis, the inverse transform also creates some errors. Panels in the bottom row show the comparison of the results of the inverse local tau-p transform. By checking the inverted wavelets in panel (e) and (f) comparing with (d), it is clear that the proposed local tau-p transform is sparser and more accurate.

MCG optimization

In this section, we propose an approach to optimize the MCG and improve the precision of multiple prediction in the local tau-p domain. Based on

SRME, the receiver-side WLRMs can be predicted by convolutions of recorded data and the primary reflections:

$$M_r(x_s,x_r,\omega) = \sum_{x_i \in \Omega} D_s(x_s,x_i,\omega)P_r(x_i,x_r,\omega) = \sum_{x_i \in \Omega} MCG(x_i,x_s,x_r,\omega) \quad . \tag{8}$$

In the frequency domain, $M_r(x_s,x_r,\omega)$ are the predicted receiver-side WLRMs for the trace with source x_s and receiver x_r. $D_s(x_s,x_i,\omega)$ and $P_r(x_i,x_r,\omega)$ are the 1D Fourier transforms of the recorded CSG and the CRG of the primary reflections, respectively. $MCG(x_i,x_s,x_r,\omega)$ is the MCG of the trace $x_s - x_r$, calculated for all the possible DRPs x_i. Ω is the summation aperture. Relying on

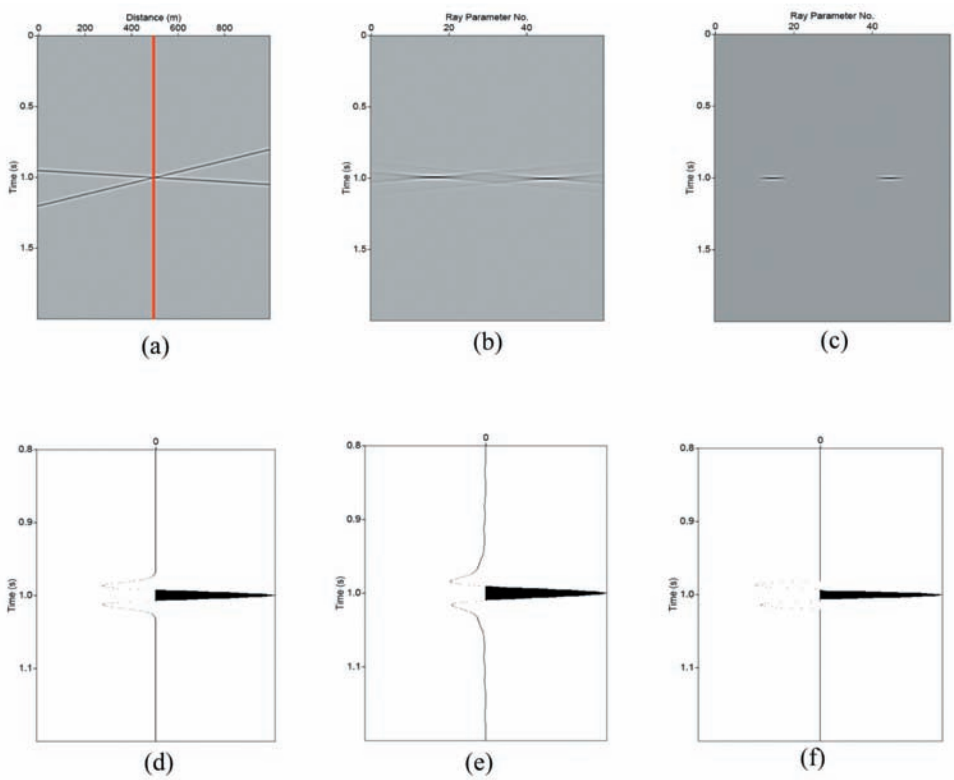

Fig. 1. Comparison between the slant stack and the proposed high-resolution transform. (a) Synthetic dataset, and the vertical line indicates the central trace of the input local window. (b) and (c) are results of the slant stack and the proposed high-resolution local tau-p transform. (d) Original record indicated by the vertical line in (a). (e) and (f) are the inverse transform of the slant stack and the proposed method.

the Huygens' Principle, all the possible DRPs are possible secondary sources that generate WLRMs. In SRME, the prediction of WLRMs involves convolution of trace couples $x_s - x_i$ and $x_i - x_r$ where x_i scans throughout any possible DRP. The convolution (or multiplication in the frequency domain, as shown in eq. (8) generates the traces of the MCG. The subsequent summation of MCG predicts the WLRMs recorded by trace $x_s - x_r$. Note that the primaries act as prediction operator to predict WLRMs. MWD replaces the prediction operator by water-layer Green's functions. With the prior information of the water-layer model, the water-layer Green's functions can be modeled through wave-equation modeling. In MWD, the receiver-side WLRMs can be predicted by:

$$M_r(x_s,x_r,\omega) = \sum_{x_i \in \Omega} D_s(x_s,x_i,\omega)G_r(x_i,x_r,\omega) = \sum_{x_i \in \Omega} MCG^m(x_i,x_s,x_r,\omega) \quad . \tag{9}$$

Compared with SRME, $G_r(x_i,x_r,\omega)$ is the CRG of the modeled Green's functions, and $MCG^m(x_i,x_s,x_r,\omega)$ is the MCG generated by MWD. In SRME or MWD, only the true DRPs are the true secondary sources that generate WLRMs. Thus only the contributions that belong to the traveltime stationary zone (Donno, 2010) contribute constructively to the prediction of WLRMs, whereas the summations of other contributions generate destructive interference.

In the local tau-p domain, we aim at optimizing the MCG through exploitations of Snell's law at the water-air interface. Assuming the surface is flat, if x_i is the true DRP, then the angle of incidence equals that of emission, as illuminated in Fig. 2a. Otherwise, this does not hold, as illuminated in Fig.2b. Therefore, the relationship between θ_1 and θ_2 can be utilized as criteria to determine the locations of stationary positions. In the local tau-p domain, the

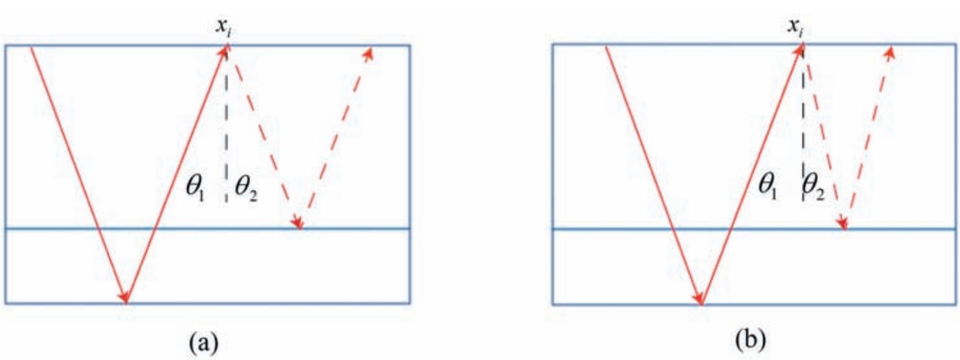

Fig. 2. Ray paths to explain how to optimize the MCG relying on Snell's law.

criteria can be represented equivalently by ray parameters. That is, when $\theta_1 = \theta_2$ holds, the corresponding relationship between ray parameters is: $p_1 = -p_2$. Based on this, the seismic data and the Green's functions of the water-layer primary reflections can be combined such that the true DRPs for different water layer-related multiple generators are automatically selected by obeying Snell's law in the local tau-p domain. For simplicity, the symbol ω is omitted in the following equations. The receiver-side WLRMs for each frequency can be predicted in the local tau-p domain by:

$$M_r(x_s,x_r,p_{i_p}) = \sum_{x_i \in \Omega} D_s(x_s,x_i,p_{i_p}) G_r(x_i,x_r,p_{n_p - i_p}) = \sum_{x_i \in \Omega} MCG(x_i,x_s,x_r,p_{i_p}) \quad , \tag{10}$$

where the range of ray parameter values is symmetric, i.e., $p_{i_p} = -p_{n_p - i_p}$, and $p_{n_p/2} = 0$. $M_r(x_s,x_r,p_{i_p})$ is the predicted receiver-side WLRMs with the ray parameter being p_{i_p}. $D_s(x_s,x_i,p_{i_p})$ is the tau-p transformed CSG, and $MCG(x_i,x_s,x_r,p_{i_p})$ is the corresponding MCG in the local tau-p domain. Here, $G_r(x_i,x_r,p_{i_p})$, the CRG of water-layer Green's functions in the local tau-p domain, act as prediction operators of receiver-side WLRMs. Relying on Snell's law, the incident local plane wave component with the ray parameter p_{i_p} is only convolved with the emitting local plane wave component with the opposite ray parameter $p_{n_p - i_p}$. Thus the artifacts caused by destructive interference are automatically removed, which results in better prediction of WLRMs. Fig. 3 explains how the receiver-side WLRMs are predicted in the local tau-p domain.

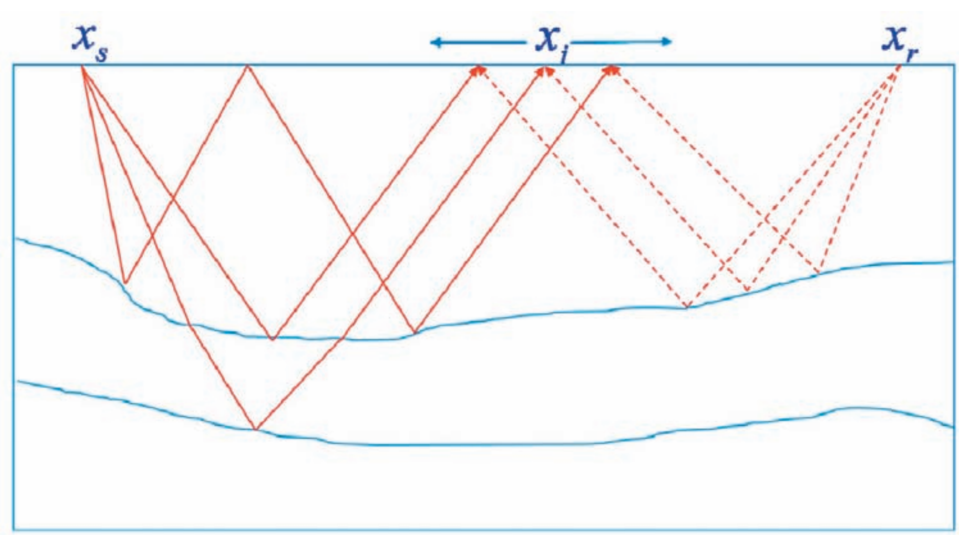

Fig. 3. Ray paths to explain how the proposed method predicts the receiver-side WLRM in the local tau-p domain.

The solid line indicates the input CSG with the ray parameter being p_{i_p}. And the dashed line indicates the prediction operator, which is the CRG of the water-layer Green's functions with the opposite ray parameter being $p_{n_p-i_p}$. The convolution of the input component with the corresponding prediction operator automatically optimizes the MCG, and thus improves the prediction precision.

According to the reciprocity principle, the source-side WLRMs can be predicted with the CRG being input and CSG of water-layer Green's functions being prediction operator, as shown by:

$$M_s(x_s,x_r,p_{i_p}) = \sum_{x_i \in \Omega} G_s(x_s,x_i,p_{i_p})D_r(x_i,x_r,p_{n_p-i_p}) \quad . \tag{11}$$

In the p-ω domain, $M_s(x_s,x_r,p_{i_p})$ is the source-side WLRMs with the ray parameter being p_{i_p}. $D_r(x_i,x_r,p_{i_p})$ is tau-p transformed CRG, and $G_s(x_s,x_i,p_{i_p})$ is the CSG of water-layer Green's functions in the local tau-p domain. Similarly, the source-receiver-side WLRMs $M_{sr}(x_s,x_r,p_{i_p})$ can also be predicted from the receiver-side, with the source-side WLRMs being input, and the corresponding CRG of Green's functions being prediction operator, as shown by:

$$M_{sr}(x_s,x_r,p_{i_p}) = \sum_{x_i \in \Omega} M_s(x_s,x_i,p_{i_p})G_r(x_i,x_r,p_{n_p-i_p}) \quad . \tag{12}$$

Lokshtanov (1999) has mentioned that a correction term should be added to correct the over-prediction of the first-order pure water-layer multiples, as given by:

$$M_w(x_s,x_r,p_{i_p}) = \sum_{x_i \in \Omega} P_w(x_s,x_i,p_{i_p})G_r(x_i,x_r,p_{n_p-i_p}) \quad . \tag{13}$$

where, $M_w(x_s,x_r,p_{i_p})$ is the first-order pure water-layer multiple. $P_w(x_s,x_i,p_{i_p})$ is the CSG of water-layer primary reflections, which can be easily separated in the local tau-p domain.

In order to demonstrate the effectiveness of multiple prediction, the proposed method is applied on synthetic data. The synthetic example is generated by 2D wave-equation modeling, and the water depth is about 100 m. Fig. 4 compares the multiples predicted by conventional MWD and the proposed method. The yellow arrows in Fig. 4b indicate the artifacts caused by interference of MCG stacking. The proposed method eliminates the artifacts, resulting in better multiple prediction. Fig. 5 compares the MCGs corresponding to the trace annotated by the solid red line in Fig. 4. In the MCG via conventional MWD, it clearly shows that the destructive interference is caused by the extended non-physical extension of the MCG tails, which creates artifacts

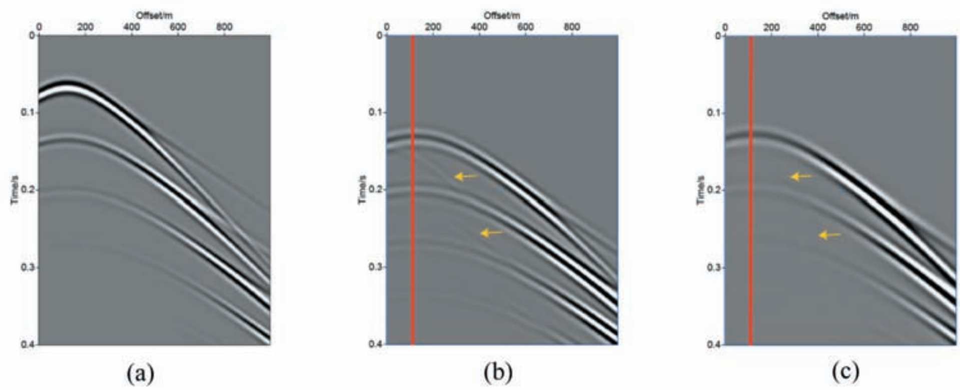

Fig. 4. Comparison of the predicted multiples by conventional MWD and the proposed method. (a) Original shot gather. (b) and (c) are WLRMs predicted by conventional MWD and the proposed method, respectively. The yellow arrows in (b) indicate the artifacts caused by destructive interference of MCG stacking.

at the edge of the aperture. In the MCG generated by the proposed method, these non-physical tails are automatically faded, and the artifacts are attenuated subsequently during multiple prediction. Figs. 5c and 5d show the stack of the MCGs generated by conventional MWD and the proposed method, respectively.

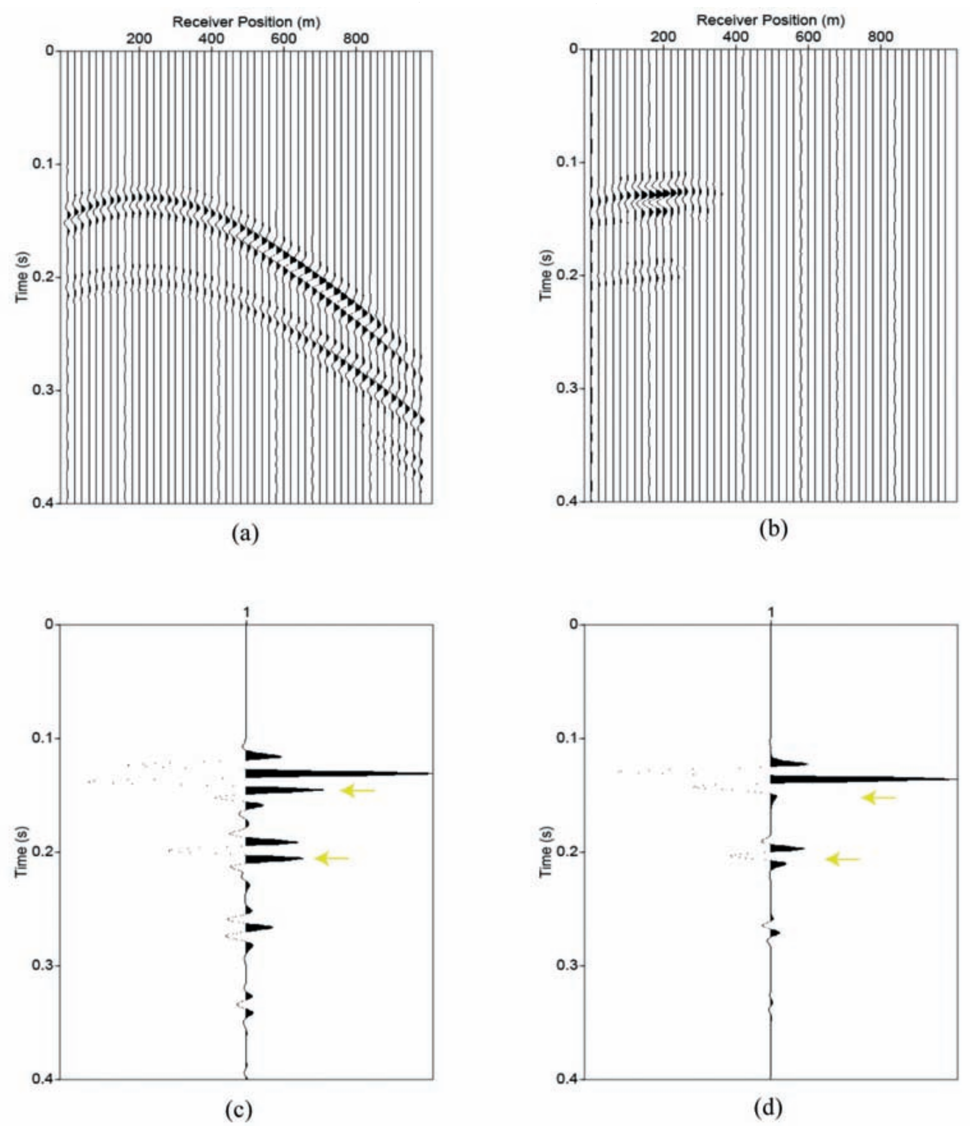

Fig. 5. Comparison of the MCGs (corresponding to the trace as annotated by the solid red line in Figs. 4b and 4c) generated by conventional MWD and the proposed method. (a) and (b) are the MCGs generated by conventional MWD and the proposed method, respectively. (c) and (d) are the stack of the MCGs in (a) and (b). The green arrows in (c) indicate the artifacts caused by deconstructive interference of the MCG, which are absent in (d).

where τ and x_k stand for intercepting time and spatial locations, and N represents the number of traces per local window. d is the input data in the space-time domain for the calculation of semblance. Semblance can be considered as the ratio of output to input energy along the proposed trajectory. Firstly, the numerator of semblance acts as the envelope of the wavelets along the trajectory, which weakens the effects of wavelet distortion during the process of subtraction. Secondly, the denominator of semblance normalizes the amplitude, which means that the value of semblance is independent of the amplitude of the arrival to be detected. These advantages can make our method more effective in multiple subtraction than the conventional methods do.

Using the semblance as constraints in the local tau-p domain, we design the filters for multiple subtraction by the following strategy: when primaries and multiples are orthogonal in the local tau-p domain, we can assign the filter with zero values where the semblance of the predicted multiples have nonzero values. Thus in the local tau-p domain, the filter for adaptive subtraction can be designed as:

$$f(\tau,p_{i_p}) = \begin{cases} 0, & \text{if } C_m(\tau,p_{i_p}) \neq 0 \\ 1, & \text{if } C_m(\tau,p_{i_p}) = 0 \end{cases} , \tag{15}$$

where $C_m(\tau,p_{i_p})$ is the semblance of the predicted multiples. It is calculated as eq. (14), with the local predicted multiples in the space-time domain used as input. Unfortunately, primaries and multiples are not always orthogonal, even in the local tau-p domain. Thus, a more generic way of designing filters is needed. Generally, we choose the Butterworth-type filter to preserve the primaries while subtracting multiples. This filter can be defined as:

$$f(\tau,p_{i_p}) = 1/\sqrt{\{1 + [C_m(\tau,p_{i_p})/\alpha C_d(\tau,p_{i_p})]^n\}} \quad . \tag{16}$$

where $C_m(\tau,p_{i_p})$ is the semblance of the original data. n acts as the parameter to control the smoothness of the filter. α is a parameter that is utilized to preserve the primaries in the local tau-p domain. When the primaries and multiples are orthogonal, the filter can suppress the multiples thoroughly, and the result is independent of α. Otherwise, α acts as a weighting factor, in order to preserve the primaries during the subtraction. In the proposed method for multiple subtraction, we first calculate the semblance in the local tau-p domain with original data and predicted multiples in the space-time domain used as input, respectively. Then, the filter for multiple subtraction is generated by eqs. (15) or (16). By applying the designed filter on the tau-p transformed original data in the local tau-p domain, the multiples can be subtracted and henceforth the primaries are obtained in the local tau-p domain. Finally, the primaries in the local tau-p domain are transformed back to the space-time domain. Thanks to the aforementioned sparse local tau-p transform, the multiples are effectively subtracted, and the primaries are preserved.

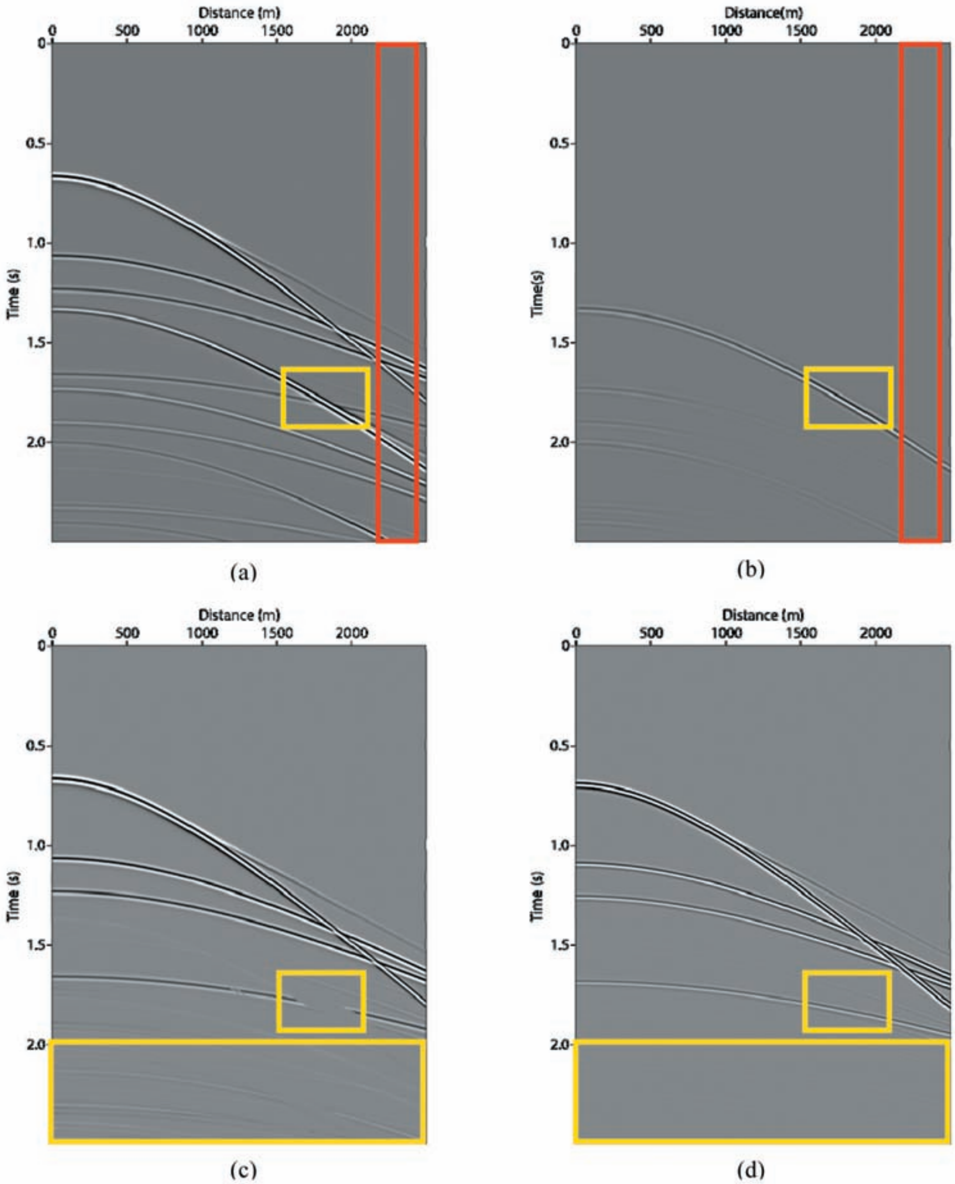

Fig. 6. Comparison of the subtraction results. (a) and (b) are the original dataset and predicted multiples generated by MWD, (c) and (d) are the subtraction results via the conventional L_2-norm and the proposed method. A 2D window of 11 traces and 400 ms is used to estimate the matching filter for conventional L_2-norm subtraction, and the matching filter length is 60 ms.

Next, we test the effectiveness of our proposed method for multiple subtraction. Without loss of generality, we tackle the areas where primaries are not orthogonal to multiples. The primaries and multiples interfere as framed by the yellow box in Figs. 6a and 6b. Comparing Figs. 6c and 6d, the conventional subtraction method based on the conventional L_2-norm cannot preserve the primaries, as shown in the yellow box in Fig. 6c. However, the proposed method can effectively eliminate the multiples and preserve the primaries at the same time, as shown in Fig. 6d. Fig. 7 shows the designed filter for multiple subtraction. Figs. 7a and 7b are the semblance of the original data and the predicted multiples, respectively. According to eq. (16), the Butterworth-type filter for multiple subtraction in the local tau-p domain is calculated, with the semblance of the original data and the predicted multiples being input. The filter is shown in Fig. 7c. Compared with Fig. 7b, the red box in Fig. 7c identifies the locations of the predicted multiples. Note that the values of the filter in the red box are almost zero. Thus when the designed filter is applied on the original data in the local tau-p domain, the multiples are adaptively subtracted.

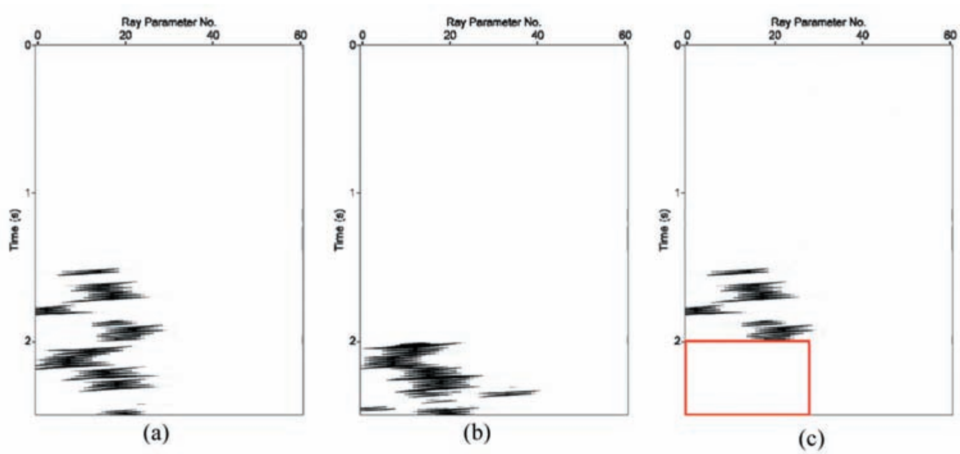

Fig. 7. Semblance of the input data and the predicted multiples and the corresponding filters for adaptive subtraction in the local tau-p domain. (a) and (b) are the semblance corresponding to the events in the red boxes in Figs. 6a and 6b, respectively, and (c) is the filter for multiple subtraction in the local tau-p domain according to eq. (16).

FIELD DATA EXAMPLES

We now validate our multiple prediction and subtraction methods by field data examples. The first example from southern China is utilized to prove the effectiveness of the proposed method for adaptive subtraction. The water bottom depth is about 1400 m. Fig. 8a shows the original dataset, and Fig. 8b shows the predicted multiples generated by MWD. The red arrows in Fig. 8a indicate that primaries and multiples interfere. Figs. 8c and 8d are the subtraction results via the conventional L_2-norm and the proposed method, respectively. Comparing Fig. 8c with 8d, the proposed method simultaneously eliminates the multiples and preserves the primaries more effectively than the conventional L_2-norm does.

Next, the proposed method for WLRM prediction and subtraction is applied on a field dataset in a shallow water case. The water bottom depth is about 80 m. Firstly, we compare the proposed method with conventional MWD through the stacked images in Fig. 9. The events indicated by blue arrows show that the proposed method works better than conventional MWD. In the prediction stage, the proposed method automatically optimizes the MCGs and thus improves the precision of multiple prediction. As a result, the proposed method generates a more accurate prediction result than the conventional MWD does. In the subtraction stage, the proposed method can not only suppress the multiples but also preserve the primaries at the same time. These advantages in both multiple prediction and subtraction make the proposed method more effective than the conventional MWD. Secondly, the effectiveness is furthermore proven through the comparisons of autocorrelation functions. In Fig. 10a, the autocorrelation functions of raw dataset shows a strong contamination by the WLRMs. Comparing Figs. 10b and 10c, we can conclude that the proposed method suppresses the WLRMs more effectively than the conventional MWD does. Finally, we draw comparisons between the proposed method and conventional MWD through the average amplitude spectra. As indicated by Fig. 11, the frequency bandwidth generated by the proposed method is broader than that generated by the conventional MWD. Therefore, the effectiveness and feasibility of the proposed method are proven, and the comparisons between the proposed method and conventional MWD also show the advantages of the proposed method.

CONCLUSIONS

A method for WLRM prediction and subtraction in the local tau-p domain is presented in this paper. Using weights in the local tau-p domain, a sparse local tau-p transform is achieved by weighted least-squares inversion. Relying on Snell's law, the Green's functions of the water-layer primary reflections in the local tau-p domain are utilized as prediction operators to optimize the MCG significantly. The true DRPs are automatically selected, thus the deconstructive interference is suppressed. As a result, the WLRM prediction is more accurate. During the subtraction stage, the semblance of the predicted WLRMs is used to identify the locations of WLRMs in the local tau-p domain. Utilizing the semblance as constraint, a Butterworth-type filter is then designed to implement

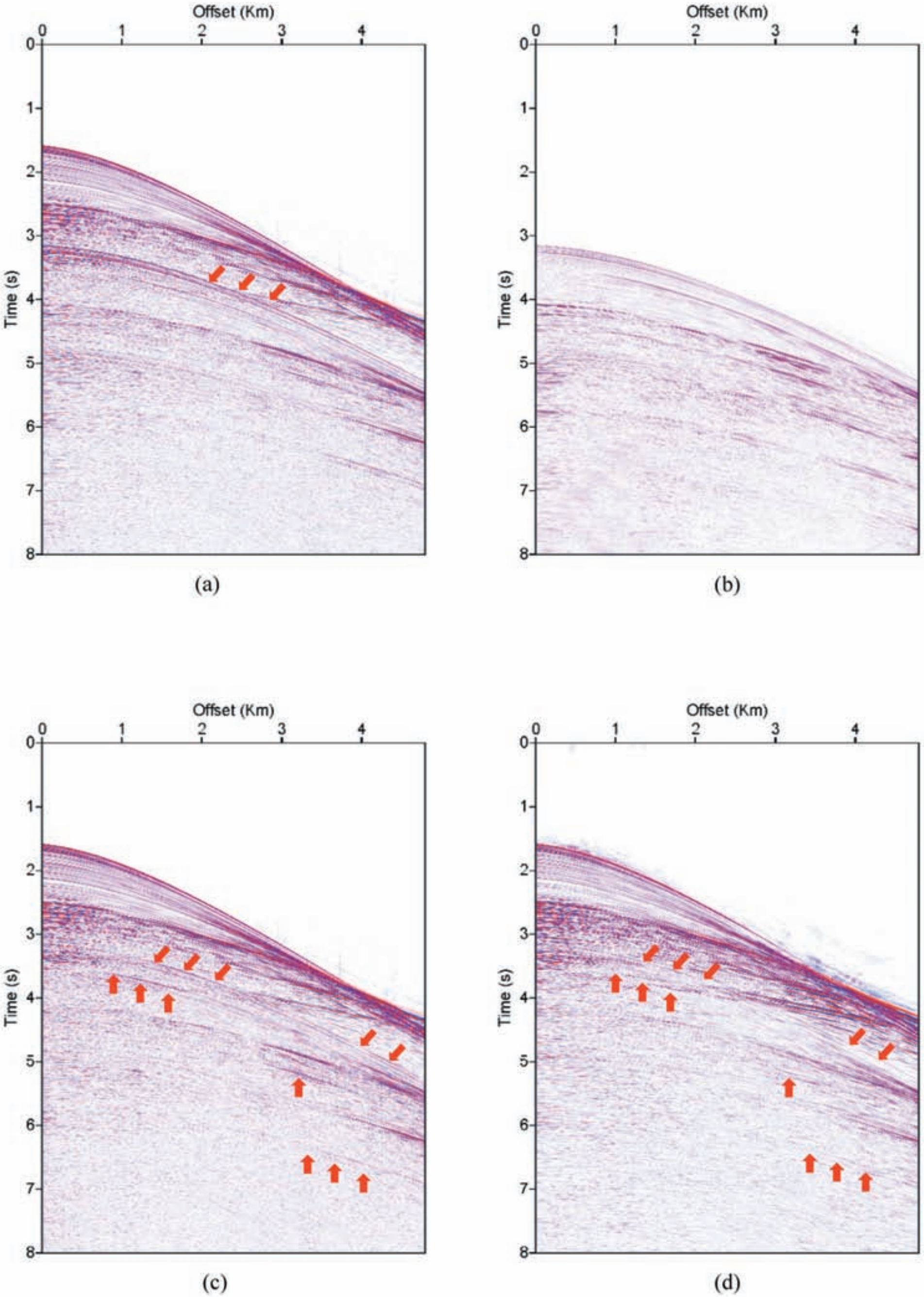

Fig. 8. Comparisons of the subtraction results for field data. (a) and (b) are the original dataset and predicted multiple generated by MWD, (c) and (d) are the subtracted results via the conventional L_2-norm and the proposed method. The red arrows prove that the proposed method subtract the multiples better than the conventional method does when the primaries and multiples interfere.

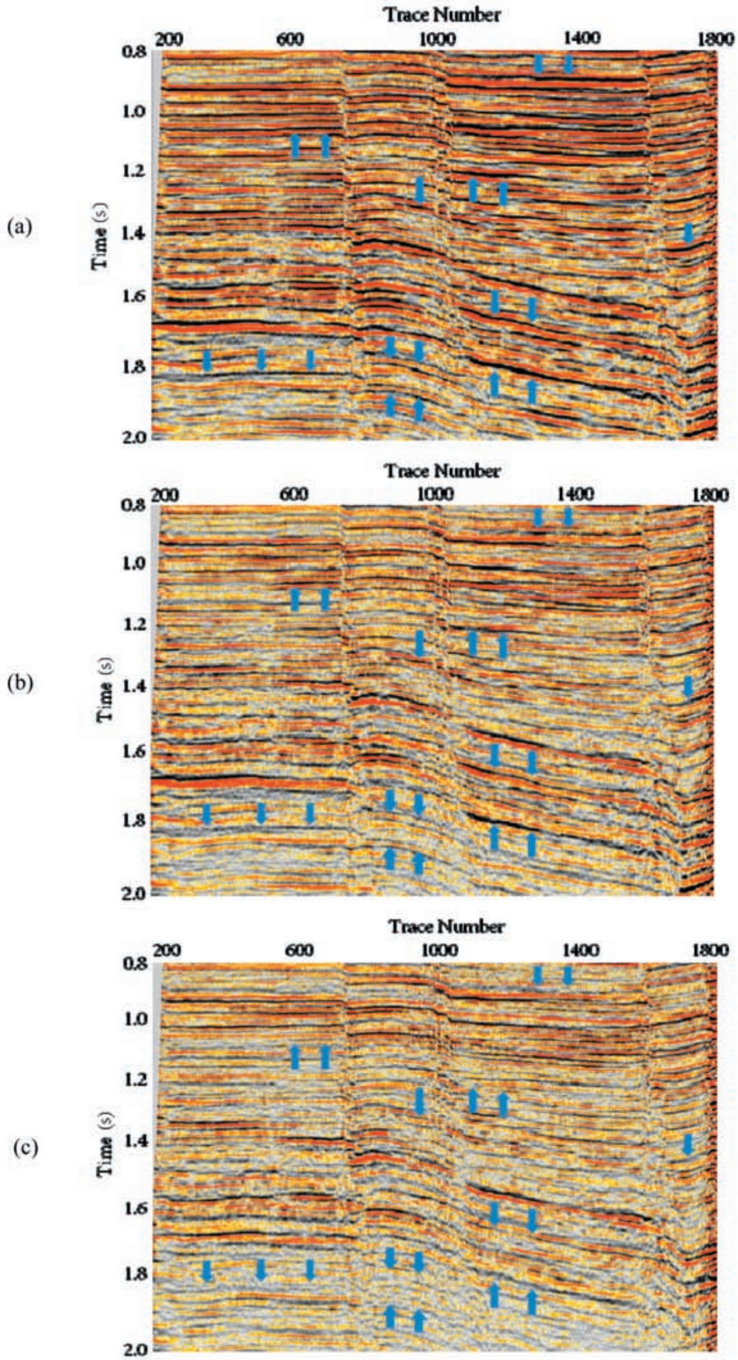

Fig. 9. Comparison of multiple removal methods via stacked images. Fig. (a) to (c) are the stacked images of raw data and the results of conventional MWD and the proposed method, respectively. The events indicated by blue arrows prove that the proposed method works better than the conventional MWD.

(a)

(b)

(c)

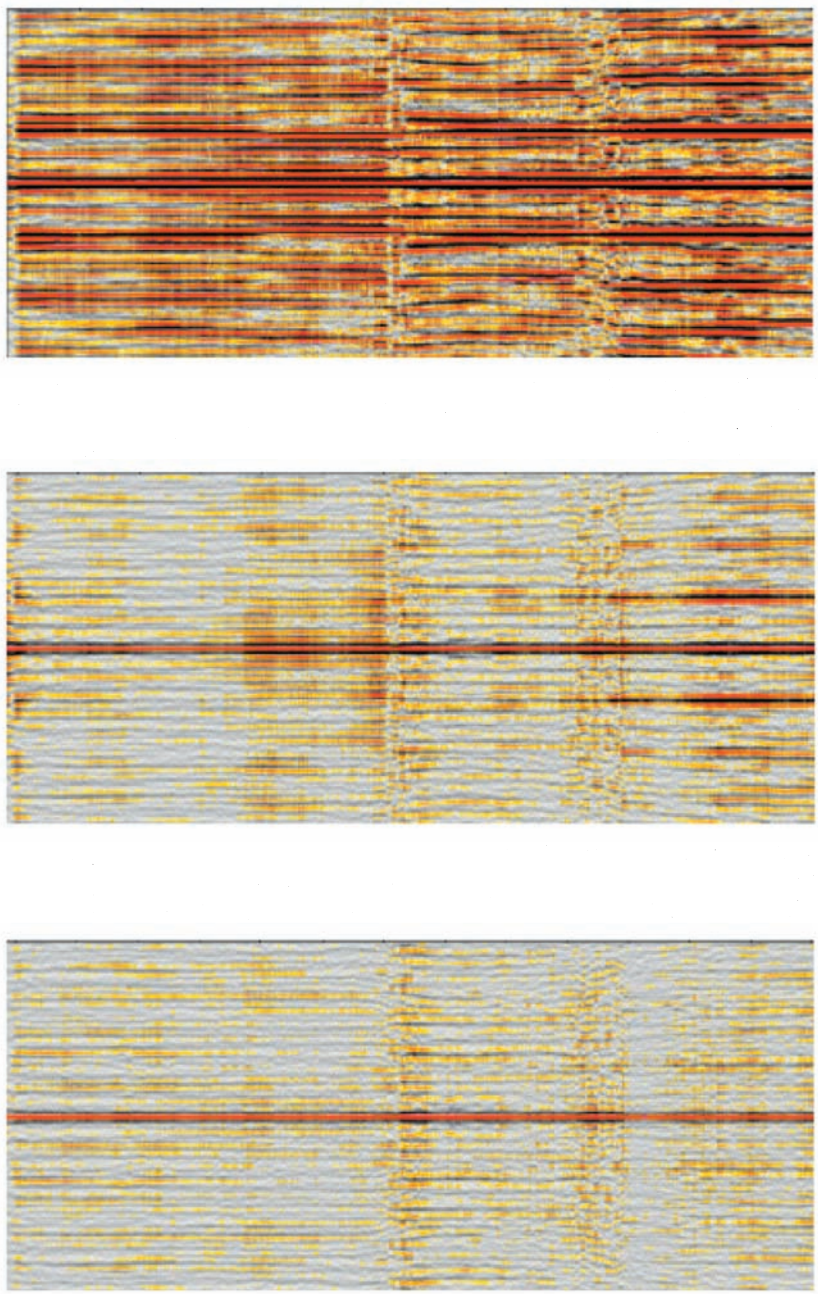

Fig. 10. Comparisons of autocorrelation functions. Fig. (a) to (c) show the autocorrelation of the raw data and the results of the conventional MWD and the proposed method, respectively.

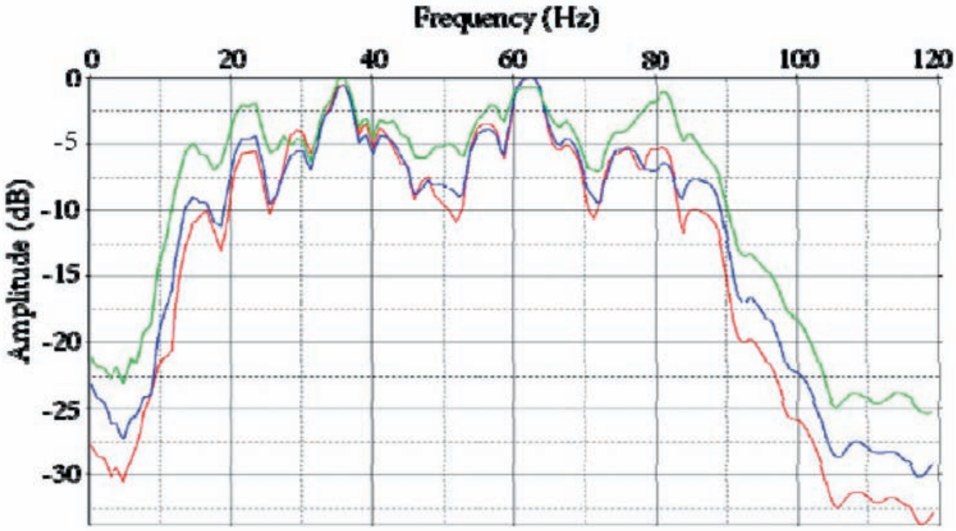

Fig. 11. Comparisons of the average amplitude spectra. Red, blue and green lines are the average amplitude spectra of raw data and the results of the conventional MWD and the proposed method, respectively.

the adaptive subtraction in the local tau-p domain. The predicted WLRMs can be effectively subtracted despite the nonorthogonality between primaries and multiples. This method not only preserves the primary energy but also weakens the effects of wavelet distortion caused by WLRM prediction. The findings of the synthetic and field data examples have proven the effectiveness and robustness of the proposed method in WLRM prediction and subtraction, and our method can serve as a solid flow for WLRM suppression.

ACKNOWLEDGEMENTS

We gratefully acknowledge the financial supports by the National Natural Science Foundation of China (41374117), '973' project (2011 CB201002) and the great and special project (2011ZX05003-003, 2011ZX05005-005-008HZ, 2011ZX05006-002).

REFERENCES

Berkhout, A.J. and Verschuur, D.J., 1997. Estimation of multiple scattering by iterative inversion, Part I: theoretical considerations. Geophysics, 62: 1586-1595.

Berryhill, J.R. and Kim, Y.C., 1986. Deep-water peg legs and multiples: Emulation and suppression. Geophysics, 51: 2177-2184.

Bienati, N., Mazzucchelli, P. and Codazzi, M., 2012. 3D-SRME antialiasing in the multiple contribution gather domain. Extended Abstr., 74th EAGE Conf., Copenhagen: Y009.

Donno, D., Chauris, H. and Noble, M., 2010. Curvelet-based multiple prediction. Geophysics, 75: 255-263.

Guitton, A. and Verschuur, D.J., 2004. Adaptive subtraction of multiples using the L_1-norm. Geophys. Prosp., 52: 27-38.

Herrmann, F.J., Wang, D. and Verschuur, D.J., 2008. Adaptive curvelet-domain primary multiple separation. Geophysics, 73: 17-21.

Keydar, S., Landa, E. and Gelchinsky, B., 1998. Multiple prediction using the homeomorphic-imaging technique. Geophys. Prosp., 46: 423-440.

Lokshtanov, D., 1999. Multiple suppression by data-consistent deconvolution. The Leading Edge, 1: 115-119. (Figures are reprinted in The Leading Edge, 1: 578-585)

Lu, W. and Liu., L., 2007. Adaptive multiple subtraction based on constrained independent component analysis. Expanded Abstr., 77th Ann. Internat. SEG Mtg., San Antonio: 2520-2524.

Monk, D.J., 1993. Wave-equation multiple suppression using constrained gross equalization. Geophys. Prosp., 41: 725-736.

Moore, I. and Bisley, R., 2006. Multiple attenuation in shallow-water situations. Extended Abstr., 68th EAGE Conf., Vienna: F018.

Spitz, S., 1999. Pattern recognition, spatial predictability, and subtraction of multiple events. The Leading Edge, 18: 55-58.

Stoffa, P.L. and Buhl, P., 1981. Direct mapping of seismic data to the domain of intercept time and ray parameter - A plane-wave decomposition. Geophysics, 46: 255-267.

Sun, W.Q. and Wang, H.Z., 2014. Model-based water-layer-related demultiple with sparse constraints. Expanded Abstr., 84th Ann. Internat. SEG Mtg., Denver: 4152-4156.

Trad, D., Ulrych, T. and Sacchi, M., 2003. Latest views of the sparse Radon transform. Geophysics, 68: 386-399.

Van Groenestijn, G.J.A. and Verschuur, D.J., 2008. Towards a new approach for primary estimation. Expanded Abstr., 78th Ann. Internat. SEG Mtg., Las Vegas: 2487-2491.

Verschuur, D.J., Wang, D. and Herrmann, F.J., 2007. Multi-term multiple prediction using separated reflections and diffractions combined with curvelet-based subtraction. Expanded Abstr., 77th Ann. Internat. SEG Mtg., San Antonio: 2535-2539.

Verschuur, D.J., 2013. Estimation of primaries by sparse inversion including the ghost. Expanded Abstr., 83rd Ann. Internat. SEG Mtg., Houston: 4094-4100.

Wang, P., Jin, H. and Xu, S., 2011. Model-based water-layer demultiple. Expanded Abstr., 81st Ann. Internat. SEG Mtg., San Antonio: 3551-3555.

Wang, Y., 2003. Multiple subtraction using an expanded multichannel matching filter. Geophysics, 68: 346-354.

Wang, Y., 2004. Multiple prediction through inversion: A fully data-driven concept for surface-related multiple attenuation. Geophysics, 69: 547-553.

Wang, Y., 2007. Multiple prediction through inversion: Theoretical advancements and real data application. Geophysics, 72: V33-V39.

Wiggins, J.W., 1988. Attenuation of complex water bottom multiples by wave equation based prediction and subtraction. Geophysics, 53: 1527-1539.

Wu, X. and Hung, B., 2013. High-fidelity adaptive curvelet domain primary-multiple separation. Extended Abstr., 75th EAGE Conf., London.